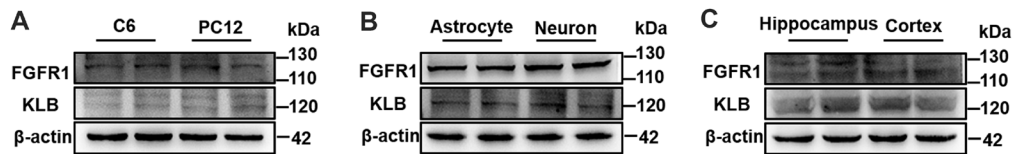


## Supplementary Information

**Figure S1.**



**Figure S1. The expression of FGFR1 and KLB in brain tissues and cells.** The expression levels of FGFR1 and KLB in C6 astrocytes and PC12 neurons (A), primary astrocytes and primary neurons (B), and brain tissues (C) were detected by western blot.

**Figure S2.**

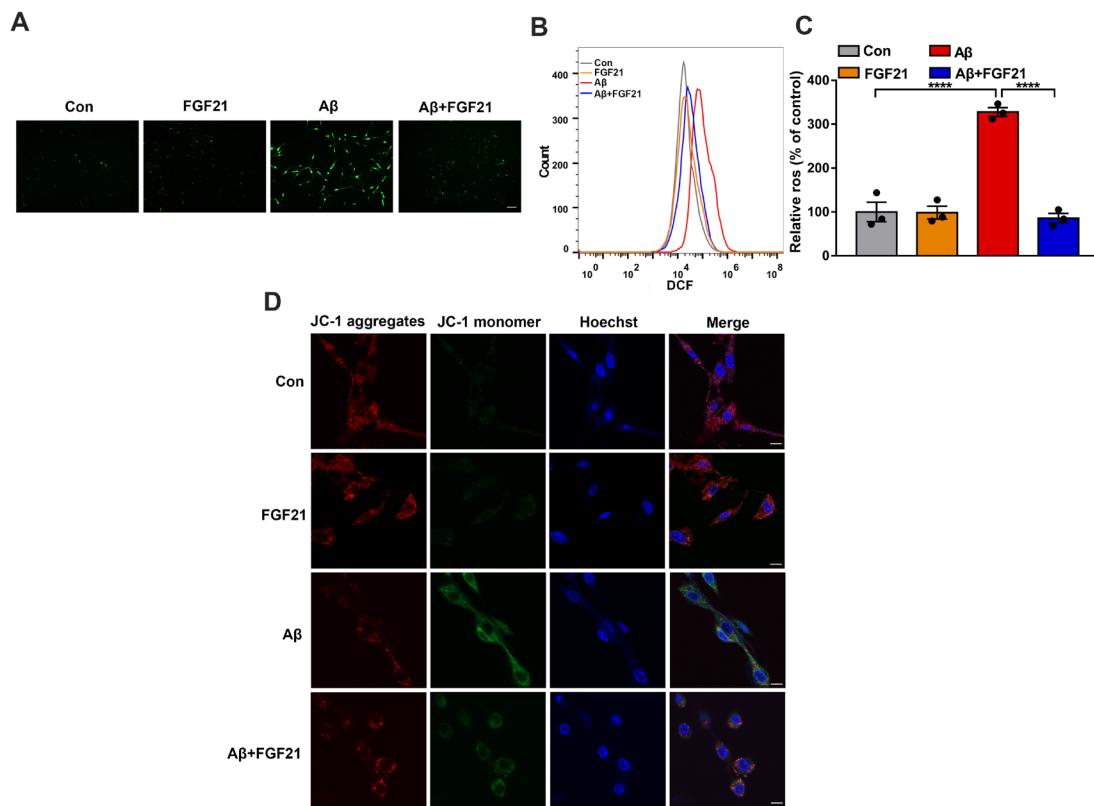


**Figure S2. Effect of FGF21 on A $\beta$ (25-35)-induced mitochondrial dysfunction in PC12 cells in a co-culture *in vitro* model.** A-B. PC12 cells in a co-culture *in vitro* model were stained with DCFH-DA probe for detection of intracellular ROS levels, and fluorescence microscopy (A) and flow cytometry (B) were used for analyses. Representative images are shown. Scale bar, 50  $\mu$ m. C. Quantitative results for B.  $n=3$ . D. PC12 cells in the *in vitro* co-culture model were stained with the JC-1 probe for detection of the mitochondrial membrane potential, and confocal laser scanning microscopy was used for analysis. Scale bar, 10  $\mu$ m. Data are presented as the mean  $\pm$  SEM. \*\*\*\*  $p < 0.0001$ .

**Figure S3.**

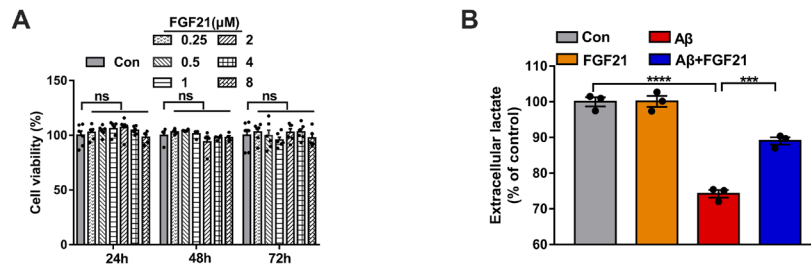


**Figure S3. Effects of FGF21 treatment alone on C6 cells, and analysis for lactate levels in medium from C6 cells treated with A $\beta$ (25-35) and/or FGF21. A.** FGF21 (0.25  $\mu$ M, 0.5  $\mu$ M, 1  $\mu$ M, 2  $\mu$ M, 4  $\mu$ M, 8  $\mu$ M) was added to C6 cells, and 24/48/72 h later, the cell viability of the C6 cells was detected by MTT assays.  $n=6$ . ns, not significant. **B.** Cells were treated with A $\beta$ (25-35) and/or FGF21, and after 48 h extracellular lactate levels in medium from C6 cells were detected.  $n=3$ . All data are presented as mean  $\pm$  SEM. \*\*\*  $p < 0.001$ ; \*\*\*\*  $p < 0.0001$ .

**Figure S4.**

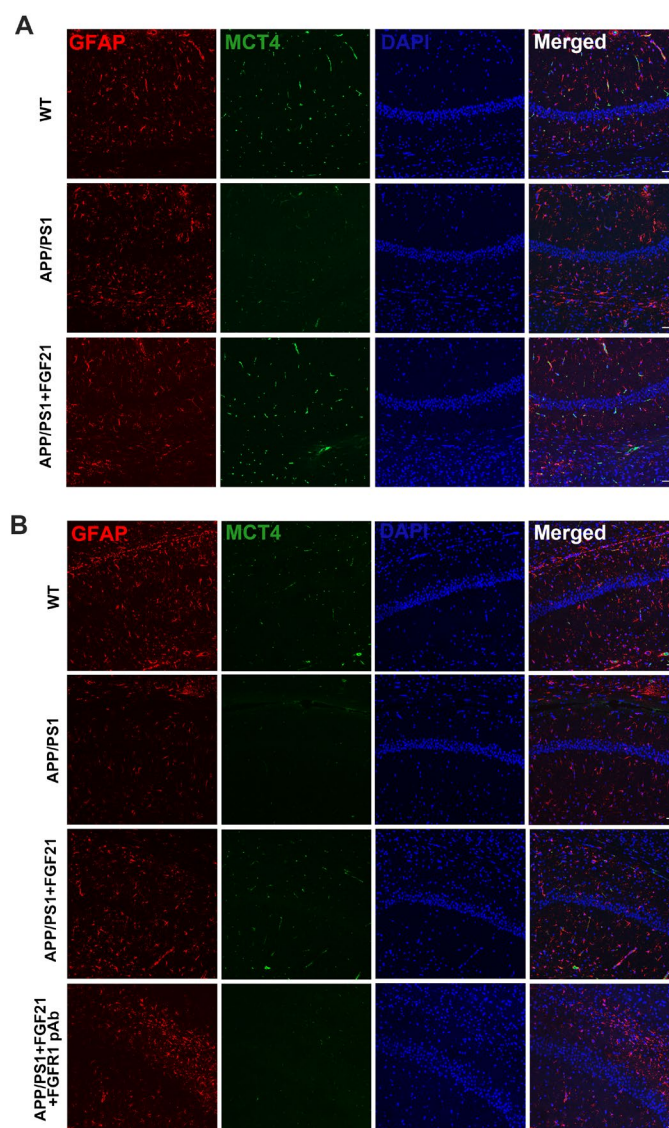


**Figure S4. Immunofluorescence staining of MCT4 in the mouse brain. A.** In peripheral administration experiments using transgenic mice, mouse brain slices were costained with anti-MCT4 antibody, anti-GFAP antibody, and DAPI. Scale bar, 50 μm. **B.** In central administration experiments using transgenic mice, mouse brain slices were costained with anti-MCT4 antibody, anti-GFAP antibody, and DAPI. Scale bar, 50 μm.

**Figure S5.**

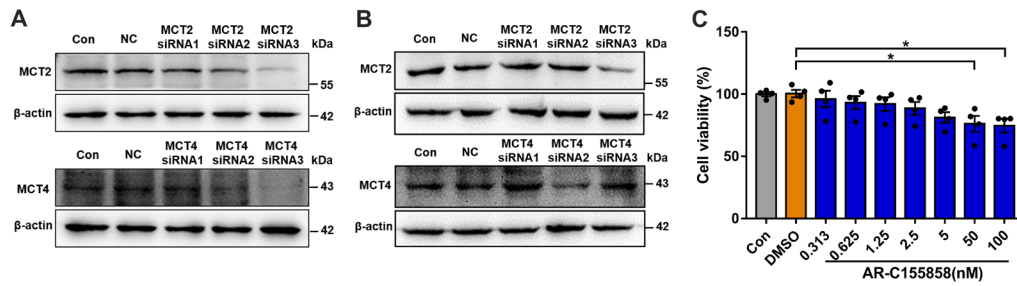


**Figure S5. Silencing efficiency test of MCT siRNA and cytotoxicity assay of**

**MCT2 inhibitor. A.** In *in vitro* transfection experiments, silencing efficiencies of

synthetic siRNAs for MCT2 and MCT4 were tested by western blot. **B.** In *in vivo*

transfection experiments, silencing efficiencies of synthetic siRNAs for MCT2 and

MCT4 were tested by western blot. **C.** Effects of different concentrations of MCT2

inhibitor (AR-C155858) on cell viability were assessed by MTT assays.  $n=4$ . Data are

presented as the mean  $\pm$  SEM. \*  $p < 0.05$ .

**Figure S6.**

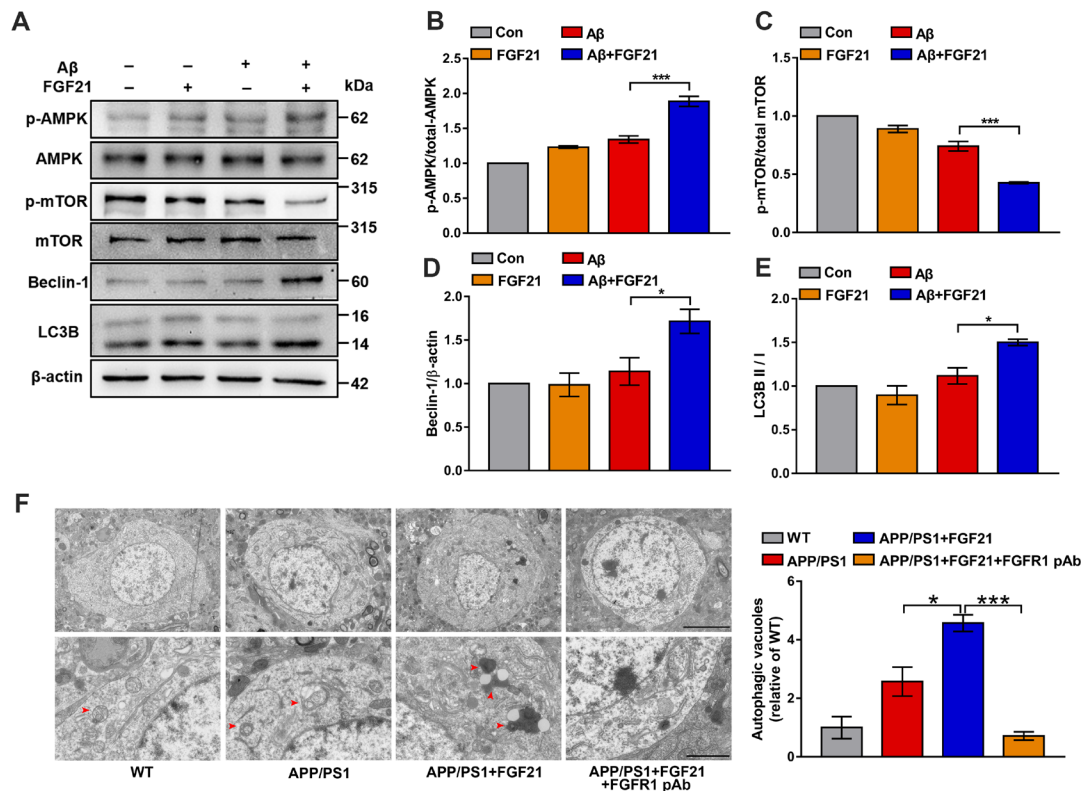


**Figure S6. Effect of FGF21 on autophagy in PC12 cells in an *in vitro* co-culture**

**model induced by Aβ(25-35).** **A.** The expression levels of p-AMPK, AMPK,

p-mTOR, mTOR, Beclin-1, and LC3B in PC12 cells co-cultured in an *in vitro* model

were detected by western blot. Representative images are shown. **B-E.** Quantitative

results for **A.**  $n=3$ . **F.** In APP/PS1 mice with/without ICV administration of FGF21 or

FGF21+FGF21 pAb, hippocampal autophagic vacuoles were analyzed using electron

microscopy. Scale bar, upper images: 5 μm, lower images: 2 μm. All data are

presented as the mean ± SEM. \*  $p < 0.05$ ; \*\*\*  $p < 0.001$ .